ELSEVIER

Modelling and simulation of anaerobic stratified biofilm for methane production and prediction of multiple steady states

Naveen Gupta [a], S.K. Gupta [a,*], K.B. Ramachandran [b]

[a] *Department of Chemical Engineering, Indian Institute of Technology, Hauz Khas, New Delhi 110016, India*

[b] *Department of Biochemical Engineering and Biotechnology, Indian Institute of Technology, Hauz Khas, New Delhi 110016, India*

Abstract

The present work deals with modelling of anaerobic metabolism in a stratified biofilm consisting of two distinct layers of microorganisms in a fixed film reactor. The model is applied to steady state conditions and is based on substrate utilization kinetics and mass transport. The model assumes that the substrate is first metabolized by the outer acidogenic layer and the subsequent products are metabolized by the inner layer of methanogens to produce finally methane and carbon dioxide. The model considers slab geometry of the biofilm, Monod kinetics for growth rate of acidogens and the inhibition effect of volatile fatty acids on growth rate of methanogens. The diffusion equations are solved simultaneously using a modified form of the technique of orthogonal collocation on finite elements to obtain concentration profiles and the rate of methane production per unit volume of the biofilm is determined. Computer simulations are carried out to study the effect of various parameters on the rate of methane production and to investigate the existence of multiple steady states. The simulation shows that for a range of parameters values three steady states exist. It is shown that the upper steady state with highest rate of methane production may lead to unsatisfactory reactor performance.

Keywords: Modelling; Simulation; Anaerobic stratified biofilm; Methane production; Steady states

1. Introduction

Water pollution is one of the crucial problems faced by the world. Anaerobic digestion is an attractive biological process for the conversion of industrial, agricultural, and domestic wastes into the very valuable energy value product methane and various volatile fatty acids. Anaerobic digestion also has other advantages over the aerobic process which are characterized by

(a) the capability of stabilizing large volumes of dilute organic slurries at low cost,

(b) low biomass production and hence a reduction in the problem of sludge disposal,

(c) a high kill rate of pathogenic micro-organisms, and

(d) the capability of producing solid residues suitable for use as a soil conditioner.

This process can be carried out by various methods. Among these the use of biofilms in tubular reactors is becoming a common practice because of the various advantages compared with other processes. Biofilm reactors can be operated at high dilution rates since the active biomass is immobilized

and retained inside the reactor as a biofilm. These biofilms can be used in trickling filters, packed bed reactors, and fluidized bed reactors. Some of the inhibition effects are reduced by the presence of diffusional limitations in the biofilm process which is not possible if the microbes are free in the liquid medium. This process also allows high volumetric organic loading rates and maintain a reasonable effluent quality. However, the existence of multiple steady states and possibility of having shock loading in the reactors brings difficulties into stable reactor operation.

The process of waste degradation has been simplified into four basic steps. These are (1) diffusion of sugars from the bulk through the stagnant liquid layer into the biofilm, (2) simultaneous diffusion and conversion of sugars into volatile fatty acids (VFAs) such as acetic acid, propionic acid, and butyric acid by a group of microorganisms called acidogens, (3) simultaneous diffusion and conversion of VFAs into methane by another group of microorganisms called methanogens, and (4) diffusion of methane from the interior of the biofilm to the bulk. Complexity of the anaerobic digestion process and the influence of mass transfer limitations and inhibition effects on the kinetics have made it difficult to understand the basic events occurring inside the system. Thus

---

* Corresponding author.

modelling and characterization of this process have brought a challenge to the biotechnological field.

An anaerobic biofilm can be of either stratified or unstratified type. In the unstratified biofilm both the acidogens and the methanogens are present as a single layer on a support particle, whereas in stratified biofilm the inner layer consists of only methanogens and the outer layer is only acidogens. Canovas-Diaz and Howell [1] developed stratified biofilm by growth in fatty acid to form the inner layer of methanogens before switching to deproteinized cheese whey water to develop the full film. Unstratified biofilm can be obtained by growing both of the organisms from the beginning in glucose medium so that they can grow simultaneously on the support particle.

Biofilm models have been developed for fixed films [2], trickling filters, packed bed reactors [3], and fluidized bed reactors [4]. All these models have assumed steady state conditions, mixed or unstratified biofilm, single substrate limiting conditions, and the effect of diffusional limitations. Modelling of stratified biofilm [5] and sequential substrate utilization in unstratified biofilm [6] have also been reported.

Droste and Kennedy [6] have developed a mathematical model based on unstratified biofilm and Monod-type reaction kinetics. They have studied the variation in effectiveness ratio with Thiele moduli. They have shown in certain circumstances that the production of intermediate substrate in the biofilm increases the conversion of primary substrate to ultimate product.

Rittman and McCarty [7,8] used the integrated technique to solve a single substrate biofilm model. They have presented their results in dimensionless form thereby increasing the generality of their plot of flux vs. bulk substrate concentration. The parameters in their plot were effective diffusivity and active depth, both in dimensionless form. The model presented by them was for a steady state biofilm in which the decaying portion continuously releases space to the growing portion such that the net biofilm thickness remains constant. According to Arcuri and Donaldson [9] this condition seems unlikely for films greater than several cells in thickness since decaying cells will be trapped underneath the younger cells.

Canovas-Diaz and Howell [5] have developed a model for stratified biofilm and compared the simulation results with experimental results already published [1]. They have shown that stratified biofilm can withstand high and inhibitory concentrations of VFAs as well as severe overloading because the outer layer acts as a protective barrier against all inhibitory compounds. They have also compared the stratified biofilm model with an unstratified biofilm model and have shown that the stratified model can explain the experimental results more accurately. However, their analysis is limited to zero-order and first-order kinetics only. Although there is an effect of inhibition of methanogens, their results do not reveal the existence of multiple steady states and this may be attributed to the use of zero- and first-order kinetics.

Substrate-inhibited reactions can have multiple operating steady states as shown by earlier workers [10,11].

Ramachandran and Kulkarni [12] have investigated the criteria for multiple steady states in immobilized-enzyme systems. The purpose of the paper was to identify the parameters for which multiple steady states exist for systems with substrate inhibition. They have also investigated the stability of these steady states. They have not considered a stratified biofilm in their analysis.

Williamson and McCarty [13] developed a biofilm model which described the substrate utilization within biofilms as a process of molecular diffusion and simultaneous biochemical reactions. The model was based on the Monod maximum utilization rate and half-velocity coefficients, the biofilm and stagnant liquid layer depths, the substrate diffusion coefficients through the biofilm and media, the biofilm density and the bulk liquid substrate concentration.

The current study is designed to show the effect of various parameters on the rate of methane production. It considers a Monod growth rate of kinetics for microorganisms together with the inhibitory effect of fatty acids on the growth rate of methanogens given by Haldane's equation. The simulation is done for a slab geometry of the biofilm. This assumption is valid for large carrier particles and thin biofilms. This assumption also reduces the complexity of the problem and hence makes analytical solution much easier to evaluate so the accuracy of the numerical scheme could be tested. Because of the inhibitory effect of the acids on the growth rate of methanogens multiple solutions may be obtained. Such an analysis can help in developing a suitable biofilm for effective operation of anaerobic biofilm reactors. The existence of multiple steady states has implications in reactor dynamics and control.

2. Theory

The model considers a stratified biofilm in slab geometry as shown in Fig. 1. All the reaction kinetics are taken to be of Michaelis–Menten type. Two basic reactions occurring are conversion of substrate sugar to fatty acids by acidogens (outer layer, zone II) and the second reaction of VFAs to methane by methanogens (inner layer, zone I). The stagnant
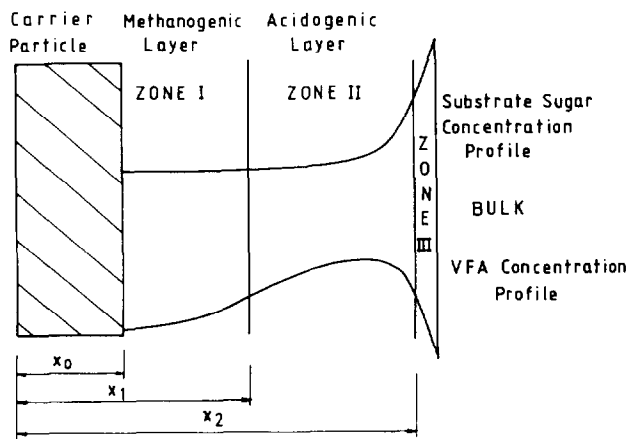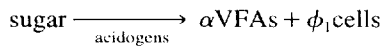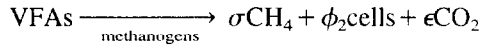

Fig. 1. Stratified biofilm.

liquid layer (zone III) also provides a diffusional limitations to the substrate. The basic reactions are as follows: for acidogenesis

$$\text{sugar} \xrightarrow[\text{acidogens}]{} \alpha\text{VFAs} + \phi_1\text{cells}$$

for methanogenesis

$$\text{VFAs} \xrightarrow[\text{methanogens}]{} \sigma\text{CH}_4 + \phi_2\text{cells} + \epsilon\text{CO}_2$$

where α, σ, ϕ_1, σ_2 and ϵ are stoichiometric parameters. All rates are normalized and measured in mass of chemical oxygen demand (COD) per unit time per unit volume of biofilm (thus $\epsilon = 0$, $\alpha + \phi_1 = 1 = \sigma + \phi_2$). The other assumptions made in the development of model are as follows.

(1) Only two reactions are taking place in series in the biofilm.

(2) The bacterial film has uniform cell density.

(3) Monod's model is applicable for cell growth.

(4) The effective diffusivities of VFAs and substrate sugar are equal. All diffusion processes are of the fickian type.

(5) Substrate concentration gradients are the only appreciable contributing factors.

(6) It is assumed that all nutrients required by the bacteria are in excess, except that which is called the limiting substrate.

(7) The system is at steady state with respect to concentration profiles in the biofilm and the biofilm thickness.

(8) All kinetics coefficients and yield factors are constant during the process.

Consider now a stratified biofilm with the outer layer of acidogens and the inner layer of methanogens. The substrate sugar diffusing into the acidogenic layer from the bulk is converted to VFAs. The differential mass balance for the transport and subsequent reaction of the substrate within the biofilm are as follows.

2.1. Acidogenic layer

$$\frac{d^2S}{dx^2} = \frac{r_s}{D_{\text{eff}}} \tag{1}$$

where r_s is equal to the rate of substrate consumption by the acidogens. The boundary conditions are

$$\text{at } x = x_1 \quad \frac{dS}{dx} = 0 \text{ and } \left(\frac{dS}{dx}\right)_{x_1^-} = \left(\frac{dS}{dx}\right)_{x_1^+} \tag{2}$$

$$\text{at } x = x_2 \quad -D_{\text{eff}}\frac{dS}{dx} = k_c(S_e - S_b) \tag{3}$$

The growth rate of microbial population is assumed to follow Monod's kinetics. Therefore for acidogens

$$\frac{dX_a}{dt} = \frac{\mu_{\text{max, a}}X_aS}{K_a + S} \tag{4}$$

We know that the yield factor for the amount of substrate conversion to acidogens is given by

$$Y_{xa/s} = -\frac{dX}{dS} = \frac{\text{mass of acidogens produced}}{\text{mass of substrate consumed}} \tag{5}$$

From Eqs. (4) and (5), the rate of substrate utilization because of biochemical reaction is given by

$$r_s = -\frac{dS}{dt} = \frac{1}{Y_{xa/s}}\frac{dX_a}{dt} = \frac{1}{Y_{xa/s}}\frac{\mu_{\text{max, a}}X_aS}{K_a + S} \tag{6}$$

$$= \frac{k_1X_aS}{K_a + S} \tag{7}$$

where

$$k_1 = \frac{\mu_{\text{max, a}}}{Y_{xa/s}} \tag{8}$$

S is the rate-limiting substrate concentration, k_1 the maximum specific rate of substrate utilization, K_a Monod's half-velocity coefficient, and X_a the acidogenic biomass. Similarly, for VFAs,

$$\frac{d^2F}{dx^2} = \frac{r_f}{D_{\text{eff}}} \tag{9}$$

where r_f is the rate of VFA consumption, and

$$Y_{f/s} = -\frac{r_f}{r_s} = \frac{\text{rate of VFA production}}{\text{rate of substrate consumption}} \tag{10}$$

The boundary conditions are

$$\text{at } x = x_1 \quad \left(\frac{dF}{dx}\right)_{x_1^-} = \left(\frac{dF}{dx}\right)_{x_1^+} \tag{11}$$

$$F_{x_1^-} = F_{x_1^+} \tag{12}$$

$$\text{at } x = x_2 \quad -D_{\text{eff}}\frac{dF}{dx} = k_c(F_e - F_b) \tag{13}$$

So, by substituting Eq. (7) in Eq. (10),

$$r_f = -Y_{f/s}r_s = -Y_{f/s}\frac{k_1X_aS}{K_a + S} \tag{14}$$

Thus the converted sugars and the VFAs diffuse into methanogenic layer (zone I). Since the sugars are not metabolized, the amount of sugar entering is equal to the amount leaving. So, the differential mass balance for sugars is given by

Methanogenic layer

$$\frac{d^2S}{dx^2} = 0 \tag{15}$$

The boundary conditions are

$$\text{at } x = x_0 \quad \frac{dS}{dx} = 0 \tag{16}$$

$$\text{at } x = x_1 \quad \left(\frac{dS}{dx}\right)_{x_1^-} = \left(\frac{dS}{dx}\right)_{x_1^+} \quad S_{x_1^-} = S_{x_1^+} \tag{17}$$

The methanogens consume the VFAs to produce methane. The growth kinetics for methanogens taking the inhibition of VFAs on methanogens into account is given by Haldane's equation

$$\frac{dX_m}{dt} = \frac{\mu_{max,\,m}X_mF}{K_m+F+F^2/K_i} \tag{18}$$

Yield factor for the amount of VFA conversion to methanogens is given by

$$Y_{xm/f} = -\frac{dX_m}{dF} = \frac{\text{mass of methanogens produced}}{\text{mass of VFAs consumed}} \tag{19}$$

So, the differential mass balance for VFAs in the methanogenic layer using Eqs. (18) and (19) is given by

$$\frac{d^2F}{dx^2} = \frac{k_2X_mF}{D_{eff}(K_m+F+F^2/K_i)} \tag{20}$$

where

$$k_2 = \frac{\mu_{max,\,m}}{Y_{xm/f}}$$

is the maximum specific rate of VFA utilization, X_m the methanogenic mass, and F the concentration of VFAs. The boundary conditions are

$$\text{at } x=x_0 \qquad \frac{dF}{dx}=0 \tag{21}$$

$$\text{at } x=x_1 \qquad F_{x_1-}=F_{x_1+} \tag{22}$$

$$\left(\frac{dF}{dx}\right)_{x_1-}=\left(\frac{dF}{dx}\right)_{x_1+} \tag{23}$$

2.3. Development of dimensionless equations

The mass balance equations and the boundary conditions (1)–(23) are made dimensionless by introducing the following dimensionless variables:

$$X=(x-x_0)/(x_2-x_0),\ Bi=K_e(x_2-x_0)/D_{eff} \tag{24}$$

$$S^*=S/S_b,\ F^*=F/F_b,\ V_1=K_a/K_m \tag{25}$$

$$T_{INHIB}=K_m/K_i \tag{26}$$

$$T_s=S_b/K_a,\ T_m=F_b/K_m \tag{27}$$

$$\alpha=x_0/(x_2-x_0) \tag{28}$$

$$Da_1=x_0^2\frac{k_1X_a}{K_aD_{eff}} \tag{29}$$

$$Da_2=x_0^2\frac{k_2X_m}{K_mD_{eff}} \tag{30}$$

where T_s and T_m correspond to the bulk concentrations of the sugars and the fatty acids respectively. The dimensionless parameter α signifies the depth of the biofilm, with the thickness of the biofilm decreasing with increase in α. T_{INHIB} is indicative of the inhibitory action of the fatty acids on the growth rate of methanogens so with increase in T_{INHIB} the inhibitory action increases. The Damkohler numbers Da_1 and Da_2 are the ratios of reaction rates and diffusion rates and can be changed by changing the activity of microorganisms. These dimensionless numbers are also functions of the thickness x_0 of the support particle and the diffusivity D_{eff} of the reactants inside the film. In the analysis x_0 and D_{eff} have been assumed to remain constant and hence the Damkohler numbers are representative of the activity of microorganisms.

Using the above dimensionless variables the mass balance equations for sugar and volatile fatty acids in different zones are given as follows.

2.3.1. Methanogenic layer

$$\frac{d^2S^*}{dX^2}=0 \tag{31}$$

The boundary conditions are

$$\text{at } X=0 \qquad \frac{dS^*}{dX}=0 \tag{32}$$

$$\text{at } X=\frac{x_1-x_0}{x_2-x_0} \qquad \left(\frac{dS^*}{dX}\right)_{X-}=\left(\frac{dS^*}{dX}\right)_{X+},\ S^*_{X-}=S^*_{X+} \tag{33}$$

$$\frac{d^2F^*}{dX^2}=\frac{Da_2}{\alpha^2}\frac{F^*}{1+T_mF^*+T_m^2T_{INHIB}(F^*)^2} \tag{34}$$

The boundary conditions are

$$\text{at } X=0 \qquad \frac{dF^*}{dX}=0 \tag{35}$$

$$\text{at } X=\frac{x_1-x_0}{x_2-x_0} \qquad F^*_{X-}=F^*_{X+} \tag{36}$$

$$\left(\frac{dF^*}{dX}\right)_{X-}=\left(\frac{dF^*}{dX}\right)_{X+} \tag{37}$$

2.3.2. Acidogenic layer

$$\frac{d^2S^*}{dX^2}=\frac{Da_1}{\alpha^2}\frac{S^*}{1+T_sS^*} \tag{38}$$

The boundary conditions are

$$\text{at } X=\frac{x_1-x_0}{x_2-x_0} \qquad \left(\frac{dS^*}{dX}\right)_{X-}=\left(\frac{dS^*}{dX}\right)_{X+},\ S^*_{X-}=S^*_{X+} \tag{39}$$

at $X= 1$ $\left(\dfrac{dS^*}{dX}\right)_X = Bi[1-(S^*)_X]$ (40)

$$\frac{d^2F^*}{dX^2} = -Y_{f/s}\frac{T_s}{T_m}\frac{Da_1}{\alpha^2}\frac{V_1 S^*}{1+T_s S^*}$$ (41)

The boundary conditions are

at $X= \dfrac{x_1-x_0}{x_2-x_0}$ $\left(\dfrac{dF^*}{dX}\right)_{X-} = \left(\dfrac{dF^*}{dX}\right)_{X+}$ (42)

$$F^*_{X-} = F^*_{X+}$$ (43)

at $X= 1$ $(dF^*/dX)_X = Bi[1-(F^*)_X]$ (44)

All the above second-order non-linear differential equations were solved simultaneously using a modified form of orthogonal collocation on finite elements [14–16] to obtain the concentration profiles of reactants and products occurring inside the biofilm. Here three-collocation-point solutions in each of the two zones have been applied since they were found to be sufficient for the solution of the differential equations. When four or more collocation point were used the results obtained were within 0.1% of the above results.

2.4. Methane production rates

The sugar consumption rate r_s per volume of biofilm and the acid consumption rate r_f per volume of biofilm were calculated from the following expressions (for slab geometry):

$$r_s = \frac{T_s K_a D_{eff}(dS^*/dX)_{X=1}}{(x_0/\alpha)^2}$$ (45)

$$r_f = \frac{T_m K_m D_{eff}(dF^*/dX)_{X=1}}{(x_0/\alpha)^2}$$ (46)

The values of concentration gradients are determined from the solution of the above differential equations. R_f can be positive if acid is being consumed or negative if the acid is being produced.

The methane production rate r_m per volume of biofilm was calculated from the expression

$$r_m = (r_s Y_{f/s} + r_f) Y_{m/f}$$ (47)

Droste and Kennedy [6] have listed the kinetic coefficient for both the acidogens and methanogens which have already been reported by various other investigators. In this simulation, the Monod half-velocity coefficients K_a and K_m for acidogens and methanogens respectively were taken to be 0.022 kg COD m^{-3} and 0.002 kg COD m^{-3}. It is assumed that the glucose concentration is very high compared to other sugars. Williamson and McCarty as well as Droste and Kennedy have considered the values of effective diffusivities of both sugars and acids inside the biofilm to be approximately 80% of their values in water. The same idea has been used in this study

and the effective diffusivities for both sugars and acids are assumed to be 0.5 cm^2 day^{-1}. The concentration of biomass in biofilm has been reported to vary from 20 to 110 kg m^{-3}. The thickness of the carrier particles was taken to be 300 μm.

2.5. Analytical solution for a limiting case

Under the limiting assumptions that T_s and T_m which represent the substrate sugar bulk concentration and VFA bulk concentration respectively approach zero, the Biot number which represents the external mass transfer resistance approaches infinity and if a slab geometry of the biofilm is assumed the mass transfer equations reduce to the following simplified forms.

2.5.1. Methanogenic layer

$$\frac{d^2S^*}{dX^2} = 0$$ (48)

The boundary conditions are

at $X= 0$ $\dfrac{dS^*}{dX} = 0$ (49)

at $X= \dfrac{x_1-x_0}{x_2-x_0}$ $\left(\dfrac{dS^*}{dX}\right)_{X-} = \left(\dfrac{dS^*}{dX}\right)_{X+}$ and $S^*_{X-} = S^*_{X+}$

(50)

$$\frac{d^2F^*}{dX^2} = \frac{Da_2}{\alpha^2} F^*$$ (51)

The boundary conditions are

at $X= 0$ $\dfrac{dF^*}{dX} = 0$ (52)

at $X= \dfrac{x_1-x_0}{x_2-x_0}$ $F^*_{X-} = F^*_{X+}$ (53)

$$\left(\frac{dF^*}{dX}\right)_{X-} = \left(\frac{dF^*}{dX}\right)_{X-}$$ (54)

2.5.2. Acidogenic layer

$$\frac{d^2S^*}{dX^2} = \frac{Da_1}{\alpha^2} S^*$$ (55)

The boundary conditions are

at $X= \dfrac{x_1-x_0}{x_2-x_0}$ $\left(\dfrac{dS^*}{dX}\right)_{X-} = \left(\dfrac{dS^*}{dX}\right)_{X-}$ and $S^*_{X-} = S^*_{X+}$

(56)

at $X = 1$ $\qquad$ $S^* = 1$ $\hspace{3cm}$ (57)

$$\frac{d^2 F^*}{dX^2} = -Y_{f/s} V_1 \frac{T_s}{T_m} \frac{Da_1}{\alpha^2} S^* \hspace{1.5cm} (58)$$

The boundary conditions are

at $X = \dfrac{x_1 - x_0}{x_2 - x_0}$ $\quad \left(\dfrac{dF^*}{dX}\right)_{X-} = \left(\dfrac{dF^*}{dX}\right)_{X+}$ $\hspace{1cm}$ (59)

$$F_{X-}^* = F_{X+}^* \hspace{3cm} (60)$$

at $X = 1$ $\qquad$ $F^* = 1$ $\hspace{3cm}$ (61)

2.6. Analytical solution

The analytical solutions of the above differential equations for sugar and VFA concentrations can be easily obtained and are given below.

2.6.1. Sugar

$$S^* = A\left(e^{\mu X} + \frac{e^{-\mu X}}{\sigma}\right) \qquad \theta < X < 1 \hspace{1cm} (62)$$

$$S^* = \text{constant} = A\left(e^{\mu\theta} + \frac{e^{-\mu\theta}}{\sigma}\right) \qquad 0 < X < \theta$$

The constants appearing in the above equations are given below:

$$\mu = (x_2 - x_0) \frac{Da_1^{1/2}}{x_0} \hspace{2cm} (63)$$

$$A = e^\mu / (e^{2\mu} + 1/\sigma) \hspace{2cm} (64)$$

$$\sigma = e^{-\mu\theta} / e^{\mu\theta} \hspace{2.5cm} (65)$$

$$\theta = (x_1 - x_0)/(x_2 - x_0) \hspace{1.5cm} (66)$$

2.6.2. Volatile fatty acids

$$F^* = C_1 X + C_2 - (\Phi A / \mu^2)(e^{\mu X} + e^{-\mu X}/\sigma)$$
$$0 < X < \theta \hspace{2.5cm} (67)$$

$$F^* = E(e^{zX} + e^{-zX}) \qquad \theta < X < 1 \hspace{1cm} (68)$$

where

$$z = Da_2^{1/2} \frac{x_2 - x_0}{x_0} \hspace{2cm} (69)$$

$$\Phi = Y_{f/s} V_1 (T_s / T_m) \, Da_1 \, \frac{(x_2 - x_0)^2}{x_0} \hspace{0.5cm} (70)$$

and the constants C_1, C_2 and E can be evaluated by solving the following equations:

$$C_1 + C_2 - (\Phi A / \mu^2)\left(e^\mu + \frac{e^{-\mu}}{\sigma}\right) = 1 \hspace{1cm} (71)$$

$$C_1 \theta + C_2 - (\Phi A / \mu^2)\left(e^{\mu\theta} + \frac{e^{-\mu\theta}}{\sigma}\right) = E(e^{z\theta} + e^{-z\theta}) \hspace{0.5cm} (72)$$

$$Ez(e^{z\theta} - e^{-z\theta}) = C_1 - (\Phi A / \mu^2)\left(e^{\mu\theta} - \frac{e^{-\mu\theta}}{\sigma}\right) \hspace{0.5cm} (73)$$

3. Results and discussion

To check the validity of the numerical scheme the analytical solution given by Eqs. (62), (67) and (68) was compared with the numerical solution for the following values of various parameters (the values of various constants are given in Table 1):

$$x_0 = 0.0003 \text{ m}$$

$$M = 0.5\%$$

carrier thickness/biofilm thickness$= 1$

$$Da_1 = Da_2 = 1$$

$$T_m = T_s = 0.0001$$

$$V_1 = 11$$

$$T_{INHIB} = 0.1$$

The concentration profiles for both sugar and the VFAs are shown in the Fig. 2, the analytical solution being compared with the numerical solution for slab geometry. We can see that exact matching between the analytical solution and the numerical solution confirms the accuracy of the numerical method used.

The numerical scheme was then applied to a range of values of the dimensionless parameters Da_1, Da_2, α, T_m. The results presented are expressed as the variation in rate of methane production as a function of Da_1 (Damkohler number for acidogens). It is also assumed that no external mass transfer effects exist, meaning that the Biot number approaches infinity.

In Figs. 3–6 for a given value of Da_1 for some cases we obtain three distinct values of methane yield. This is observed because of the inhibitory effect of VFAs on the growth rate of methanogens as given by Haldane's equation. Because of inhibition the rate of consumption of VFAs first increases with increase in concentration of VFA and after reaching a threshold value it starts decreasing. The steady states correspond to intersection of the rate of diffusion curve and the rate of consumption curve for the VFAs. The highest yield
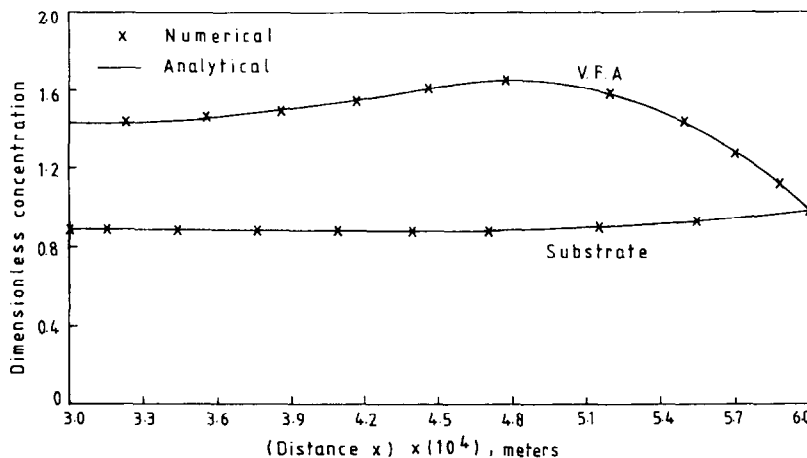
Fig. 2. Comparison of concentration profiles for VFAs and sugar for the analytical and the numerical solutions.

corresponds to a negative concentration profile of the VFAs which is not physically possible. Therefore the biofilm cannot exist at that steady state. The intermediate point is the meta-stable steady state. Since on slight decrease in concentration the rate of diffusion will be less than the rate of consumption, the concentration will further decrease and the biofilm will be stable at the uppermost steady state. The reverse will be the case if the concentration of VFA increases and the biofilm will be stable at the lowermost steady state. The lowermost steady state is dynamically stable as slight shifts in concentration will return the biofilm to the lowermost steady state.

In the initial studies the biofilm is assumed to be present somewhere in the middle of the tubular reactor. So the bulk concentrations of the sugar and the acid were assumed to be average of the inlet and the outlet concentrations in the reactor. Thus the T_s and T_m values were chosen to be 200 and 100 respectively.

Fig. 3 shows the effect of Damkohler number Da_1 for sugars and the relative thickness of both the acidogenic and the methanogenic layers on the methane production rate. The values of Da_2 and $x_0/(x_2-x_0)$ are chosen to be 150 and 0.3 respectively. At low values of Da_1 the methane production rate appears to be high. With the increase in the value of Da_1 the acid production rate inside the biofilm increases and hence

the concentration of acid increases throughout the film. Because of this the acid inhibition effect on the methane production increases and so the methane production decreases with increase in Da_1.

Within a certain range of Da_1 multiple steady states are obtained for the process and that range varies for different degrees of stratification. At all the steady state points the acid consumption rates are equal to the acid diffusion rates. The top and the bottom steady states are dynamically stable while the middle steady state is metastable. It is observed from Fig. 3 that when the thickness of the methanogenic layer is increased while the total thickness of the biofilm is kept constant the methane production rate increases. This happens for two reasons. One is the increase in the methanogenic population and the other is the decrease in acid inhibition effect since decreasing the thickness of the acidogenic layer leads to the decrease in the acid production inside the biofilm.

In actual practice, the value of the Damkohler number changes continuously during the reactor operation because of continuous growth and death of the microbes. This change has a marked effect on the reactor's stability. For example, if the methanogenic layer thickness is 80% of the total biofilm and Da_1 decreases from 80 to 75 during the process, then it is very difficult to guess which steady state the biofilm will
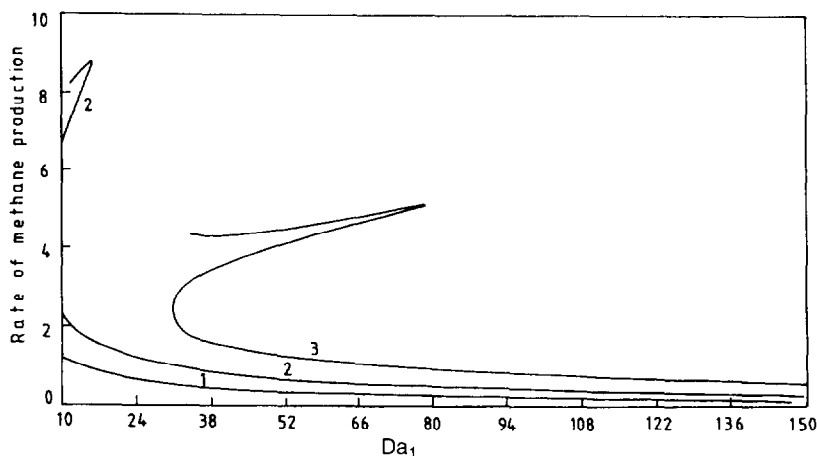

Fig. 3. Effect of Da_1 and relative thickness of both of the layers on methane production rate for $\alpha = 0.3$, $Da_2 = 150$, $T_s = 200$, $T_M = 100$ and the following methanogenic populations: curve 1, $M = 0.4\%$; curve 2, $M = 0.6\%$; curve 3, $M = 0.8\%$.
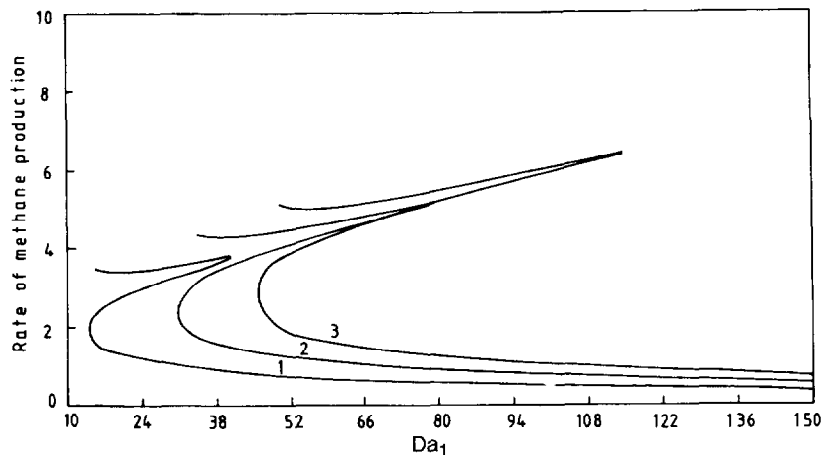
Fig. 4. Effect of Da_2 on methane production rate for $\alpha = 0.3$, $M = 0.8\%$, $T_s = 200$, $T_M = 100$ and the following values of Da_2: curve 1, 100; curve 2, 150; curve 3, 200.

finally go to. Therefore it is wise to do a dynamic study of the biofilm.

The effect of Da_2 on the methane production rate has been shown in Fig. 4. In this study, the thickness of the methanogenic layer is assumed to be 80% of the total biofilm thickness. It is observed from Fig. 4 that increases in Da_2 lead to more methane production. This is obvious since the conversion of acid to methane becomes faster as the rate of reaction increases. Again multiple steady states are observed for all three values of Da_2.

Fig. 5 shows the variation in methane production rate with $\alpha = x_0 / (x_2 - x_0)$, which signifies the depth of the biofilm. An interesting observation is made when the three biofilms are compared. For low value of Da_1 a biofilm with $x_0 / (x_2 - x_0)$ equal to 0.4 produces more methane than a biofilm with $x_0 / (x_2 - x_0)$ equal to 0.7 but for higher values of Da_1 the thinnest biofilm becomes the highest methane producer. The reasons for such an observation are not very obvious. Many factors contribute to produce such an effect such as reaction order, diffusional limitation and an inhibition effect. The parameter $x_0 / (x_2 - x_0)$ not only affects the mass balance equation but also appears in the rate expressions since all rates are calculated on a per unit volume basis.
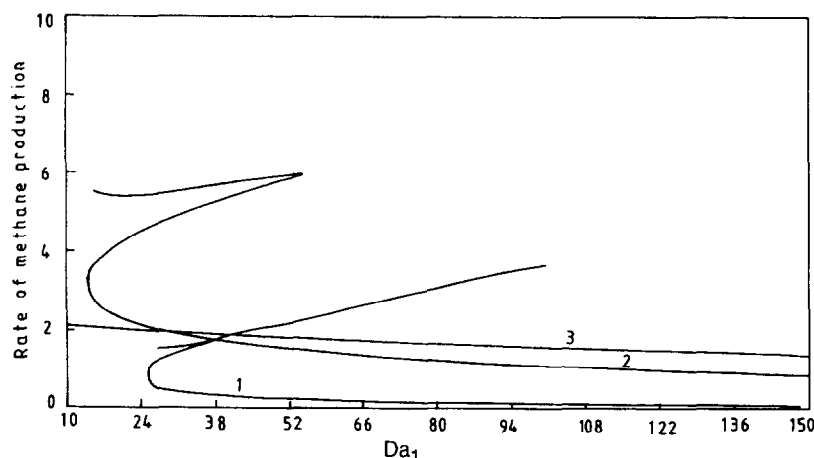
3.1. Behaviour of the biofilm at the inlet of the tubular reactor

The analysis in the previous section was based on the assumption that the biofilm is exposed to concentrations of sugar and acid which are normally observed somewhere in the middle of the reactor. Waste water usually contains a very high concentration of sugar and a very low concentration of acids. So the biofilm present at the inlet of a tubular reactor is exposed to incoming waster water and that at the outlet is exposed to low concentrations of sugar and acids. Before a reactor model is developed it is very important to analyse the behaviour of a stratified biofilm under these conditions.

Fig. 6 shows the methane-producing capability of the biofilm present at the inlet of the reactor. Here T_m is varied from a low value of 25 to a high value of 125. It can be seen from the figure that at low values of T_m the methane production rates are higher, this can be attributed to a reduced inhibitory effect of VFAs on the methanogens.

In Figs. 3–6 we have observed that the highest yield is not physically possible because of the negative concentration of VFA predicted by the numerical scheme used over a certain thickness of the biofilm. This shows that reactor failure can
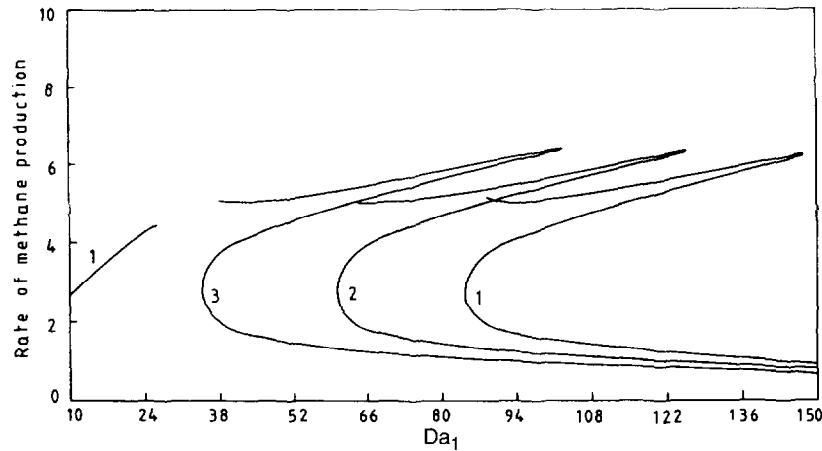

Fig. 5. Effect of α on methane production rate for $M = 0.8\%$, $Ga_2 = 150$, $T_s = 200$, $T_M = 100$ and the following values of α: curve a, 0.1; curve 2, 0.4; curve 3, 0.7.

Fig. 6. Effect of T_m on methane production rate for $\alpha = 0.3$, $M = 0.8\%$, $Da_2 = 200$, $T_s = 200$ and the following values of T_m: curve 1, 25; curve 2, 75; curve 3, 125.

occur during the operational fluctuations as the nutrient concentration is not sufficient to support the biofilm thickness which is assumed to remain constant.

4. Conclusions

Before a biofilm reactor is designed, it is important to study the behaviour of biofilms under various conditions. For a stratified biofilm, the Damkohler numbers Da_1 and Da_2, α, and the relative layer thickness should be optimized. This analysis also gives a good understanding of the multiple steady state phenomena occurring in biofilms. It is also observed that reactor failure can occur if the steady state shifts to the higher steady state which in the current study corresponds to a negative concentration profile of VFAs over a certain thickness of the biofilm. This sudden shift can occur because of fluctuations in Damkohler number caused by the continuous growth and decay of microorganisms.

Table 1
Numerical values of various constants used in the solution

D_{eff}	=	$5.787 \text{ m}^2 \text{ s}^{-1}$
K_a	=	$0.022 \text{ kg COD m}^{-3}$
K_m	=	$0.002 \text{ kg COD m}^{-3}$
K_i	=	$0.02 \text{ kg COD m}^{-3}$
x_0	=	0.0003 m
$Y_{f/s}$	=	0.8
$Y_{m/f}$	=	0.8

Appendix A: Nomenclature

Bi   Biot number (dimensionless)
D_{eff} effective diffusivity ($\text{m}^2 \text{ s}^{-1}$)
Da_1 Damkohler number for sugars (dimensionless)
Da_2 Damkohler number for acids (dimensionless)
F concentration of VFA at any x (kg COD m^{-3})
F^* F/F_b, dimensionless VFA concentration

F_b concentration of VFA in bulk (kg COD m^{-3})
F_e concentration of VFA at $x = x_2$ (kg COD m^{-3})
K_a Monod half-velocity coefficient for acidogens (kg COD m^{-3})
K_i acid inhibition coefficient of Haldane equation (kg COD m^{-3})
K_m Monod half-velocity coefficient for methanogens (kg COD m^{-3})
k_1 maximum specific substrate uptake rate of acidogens (h^{-1})
k_2 maximum specific substrate uptake rate of methanogens (h^{-1})
k_c external mass transfer coefficient (m s^{-1})
M methanogenic population (%)
r_f rate of VFA consumption ($\text{kg COD m}^{-3} \text{ s}^{-1}$)
r_s rate of substrate sugar consumption ($\text{kg COD m}^{-3} \text{ s}^{-1}$)
S concentration of substrate sugar at any x (kg COD m^{-3})
S^* S/S_b, dimensionless substrate concentration
S_b concentration of substrate sugar in bulk (kg COD m^{-3})
S_c concentration of substrate sugar at x_2 (kg COD m^{-3})
T_{INHIB} ratio of K_m and K_i (dimensionless)
T_m ratio of F_b and K_m (dimensionless)
T_s ratio of S_b and K_a (dimensionless)
V_1 ratio of K_a and K_m (dimensionless)
X $(x - x_0)/(x_2 - x_0)$, dimensionless radius
X_a acidogenic biomass (kg COD m^{-3})
X_m methanogenic biomass (kg COD m^{-3})
x distance from the centre of the carrier particle to any point in the biofilm (cm)
x_0 radius of sand particle (cm)
x_1 radius of sand particle and methanogenic layer combined (cm)
x_2 radius of sand particle and methanogenic layer and acidogenic layer combined (cm)
$Y_{f/s}$ mass of VFA produced by mass of substrate consumed
$Y_{m/f}$ mass of methane produced by mass of acid consumed

Greek letters

α ratio of the support and biofilm thickness (dimensionless)

$\mu_{max,a}$ maximum growth rate of acidogens ($m^3 s^{-1}$)

$\mu_{max,m}$ maximum growth rate of methanogens ($m^3 s^{-1}$)

References

[1] M. Canovas-Diaz and J.A. Howell, *Biotechnol. Lett.*, *8* (1986) 379.

[2] F.B. DeWalle and E.S.K. Chain, *Biotechnol. Bioeng.*, *18* (1986) 1275.

[3] A.D. Meurnier and K.J. Williamson, *J. Environ. Eng. Div. ASCE*, *107* (1981) 307.

[4] G.F. Andrews, *Biotechnol. Bioeng.*, *24* (1982) 2013.

[5] M. Canovas-Diaz and J.A. Howell, *Biotechnol. Bioeng.*, *32* (1988) 348.

[6] K.J. Kennedy and R.L. Droste, *Biotechnol. Bioeng.*, *28* (1986) 1713.

[7] B.E. Rittman and P.L. McCarty, *Biotechnol. Bioeng.*, *22* (1980) 2343.

[8] B.E. Rittman and P.L. McCarty, *Biotechnol. Bioeng.*, *22* (1980) 2359.

[9] E.J. Arcuri and T.L. Donaldson, *Biotechnol. Bioeng.*, *23* (1981) 2149.

[10] D.J. Wadiak and R.G. Carbonell, *Biotechnol. Bioeng.*, *17* (1975) 1761.

[11] J.C. Van Den Heuvel and H.H. Beeftink, *Biotechnol. Bioeng.*, *31* (1988) 718.

[12] P.A. Ramachandran and B.D. Kulkarni, *Biotechnol. Bioeng.*, *22* (1980) 1759.

[13] K. Williamson and P.L. McCarty, *Biotechnol. Bioeng.*, *22* (1980) 2343.

[14] B.A. Finlayson, *Non-linear Analysis in Chemical Engineering*, Tata–McGraw-Hill, New York, 1980.

[15] N. Gupta, *B. Tech. Project Thesis*, Department of Chemical Engineering, IIT Delhi, 1995.